

The influence of the external flow rates on an absorption chiller

Yuri R. Fischer^{*a}, Italo S. Silva^a, José C. C. Dutra^a

^{*a} Department of Mechanical Engineering, Federal University of Pernambuco, Recife, Brazil

Correspondence Author: Yuri R. Fischer, *Department of Mechanical Engineering, Federal University of Pernambuco, Recife, Brazil*

Received date: 15 July 2019, Accepted date: 28 September 2019, Online date: 30 September 2019

Copyright: © 2019 Fischer *et al.*, This is an open-access article distributed under the terms of the Creative Commons Attribution License, which permits unrestricted use, distribution, and reproduction in any medium, provided the original author and source are credited.

Abstract

The variation of the nominal chiller flow rates can cause different effects in absorption chiller performance. In the present work, a thermodynamic modeling of a single effect absorption chiller was developed based on mass, energy and species balances in steady state condition to analyze the effects of the external flow rates in this chiller. The increase of the hot water flow rate or the cooling water flow rate produces better performance of the chiller. If the chilled water flow rate decreases the performance improves also. In the flow rates range analyzed of the chiller, the best performance configuration is with 120% of hot water flow rate and the cooling water flow rate, and 80 % of chilled water flow rate. Higher inlet hot water temperatures result in higher coefficient of performance (COP) and heat removed as well as lower inlet cooling water temperature.

Key words: Absorption; Chiller; Flow rate; Performance.

INTRODUCTION

Many industrial processes use thermal energy from burning fossil fuel to produce steam or heat and, in general, heat is rejected to surrounding as waste after these processes (Srikhirin *et al.*, 2001). This waste of heat can be converted to a useful absorption refrigeration cycle, which can reduce the electricity consumed in conventional refrigeration and help to reduce environmental problems related to the combustion fossil fuels and production of electricity. (Srikhirin *et al.*, 2001).

The system which increases the efficiency of energy uses by the simultaneous production of power and heat energy from one system is called as cogeneration or combined heat and power (CHP) (Lee *et al.*, 2019). The absorption chiller is the equipment which produces cold water for refrigeration by heat recovery through one or more effects. The chiller that uses water/lithium bromide (H₂O/LiBr) solution is one of the most present in absorption systems.

Chahartaghi *et al.* (2019) observed that many studies have been done on the analysis and modeling of absorption chillers with series and parallel flow, however there are few studies that can compare these systems in various operating conditions. External flow rates are a parameter that may be important for the performance control of an absorption chiller. Robust and simple control is important for a safe and efficient absorption chillers operation (Meyer; Ziegler, 2019).

In the present paper, was realized a modelling of a single-effect lithium bromide absorption chiller using mass, energy and species balances in steady state condition and was analyzed the influence of external flow rates on this chiller.

MODELING OF THE SINGLE-EFFECT ABSORPTION CHILLER

A single-effect absorption chiller modelling was done with all the balances equations programmed in the software EES (Engineering Equation Solver) considering the steady state condition. The balances of mass, energy and species were made for each component of the absorption chiller. Fig. 1 presents the absorption chiller modeled and its points.

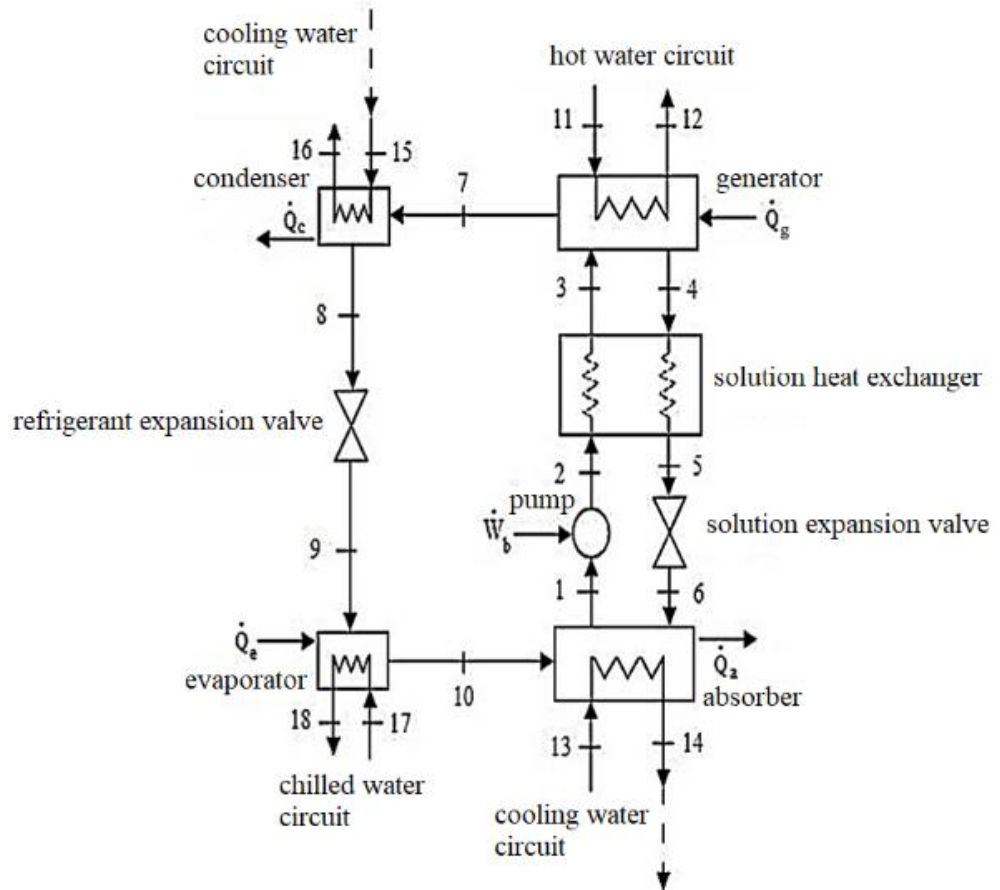


Figure 1: Single-effect absorption chiller.

Some simplifying assumptions are adopted in the developed modeling:

- The internal components of the chiller do not exchange heat with the external environment;
- Only water (0% LiBr) runs through the refrigerant circuit at points 7, 8, 9, 10;
- The variations of kinetic energy and potential of the system are considered negligible;

Table 1 shows the modelling equations obtained in the steady state condition.

Table (1): Modelling equations in steady state condition.

Chiller component	Mass balance	Title Text	Title Text
Generator	$\dot{m}_3 = \dot{m}_4 + \dot{m}_7$ $\dot{m}_{11} = \dot{m}_{12}$	$\dot{Q}_G = \dot{m}_4 h_4 + \dot{m}_7 h_7 - \dot{m}_3 h_3$ $\dot{Q}_G = \dot{m}_{11} \cdot (h_{11} - h_{12})$	$\dot{m}_3 x_3 - \dot{m}_4 x_4 - \dot{m}_7 x_7 = 0$
Condenser	$\dot{m}_7 = \dot{m}_8$ $\dot{m}_{15} = \dot{m}_{16}$	$\dot{Q}_C = \dot{m}_7 \cdot (h_7 - h_8)$ $\dot{Q}_C = \dot{m}_{15} \cdot (h_{16} - h_{15})$	-
Refrigerant expansion valve	$\dot{m}_8 = \dot{m}_9$	$h_8 = h_9$	-
Evaporator	$\dot{m}_9 = \dot{m}_{10}$ $\dot{m}_{17} = \dot{m}_{18}$	$\dot{Q}_E = \dot{m}_{10} \cdot (h_{10} - h_9)$ $\dot{Q}_E = \dot{m}_{17} \cdot (h_{17} - h_{18})$	-
Absorber	$\dot{m}_1 = \dot{m}_{10} + \dot{m}_6$ $\dot{m}_{13} = \dot{m}_{14}$	$\dot{Q}_A = \dot{m}_{10} h_{10} - \dot{m}_1 h_1 + \dot{m}_6 h_6$ $\dot{Q}_A = \dot{m}_{13} \cdot (h_{14} - h_{13})$	$\dot{m}_{10} x_{10} - \dot{m}_1 x_1 + \dot{m}_6 x_6 = 0$

Chiller component	Mass balance	Title Text	Title Text
Solution pump	$\dot{m}_1 = \dot{m}_2$	$\dot{W}_{bs} = \dot{m}_1 h_1 - \dot{m}_2 h_2$	$x_1 = x_2$
Solution heat exchanger	$\dot{m}_2 = \dot{m}_3$ $\dot{m}_4 = \dot{m}_5$	$\dot{Q}_{tcs} = \dot{m}_3 \cdot (h_3 - h_2)$ $\dot{Q}_{tcs} = \dot{m}_4 \cdot (h_4 - h_5)$	$x_2 = x_3$ $x_4 = x_5$
Solution expansion valve	$\dot{m}_5 = \dot{m}_6$	$h_5 = h_6$	-

The efficiency equation of the solution heat exchanger in the chiller found from the balances is:

$$\varepsilon = \frac{T_4 - T_5}{T_4 - T_2}$$

The input data of the modeling is collected from the manufacturer datasheet of a 10 TR single-effect lithium bromide absorption chiller. Table 2 presents the principal nominal data provided by the manufacturer datasheet.

Table (2): Modelling equations in steady state condition.

	Temperature [°C]	Flow rate [kg/s]
Inlet hot water	88	2,4
Inlet cooling water	31	5,1
Outlet chilled water	7	1,52

Thus, with the input data and equations, the modeling can show the results.

RESULTS AND DISCUSSION

The effects of each external flow rate on the COP and heat removed (\dot{Q}_E) and on the heat removed are analyzed. Fig. 2 shows the graph COP versus hot water flow rate (\dot{m}_{11}).

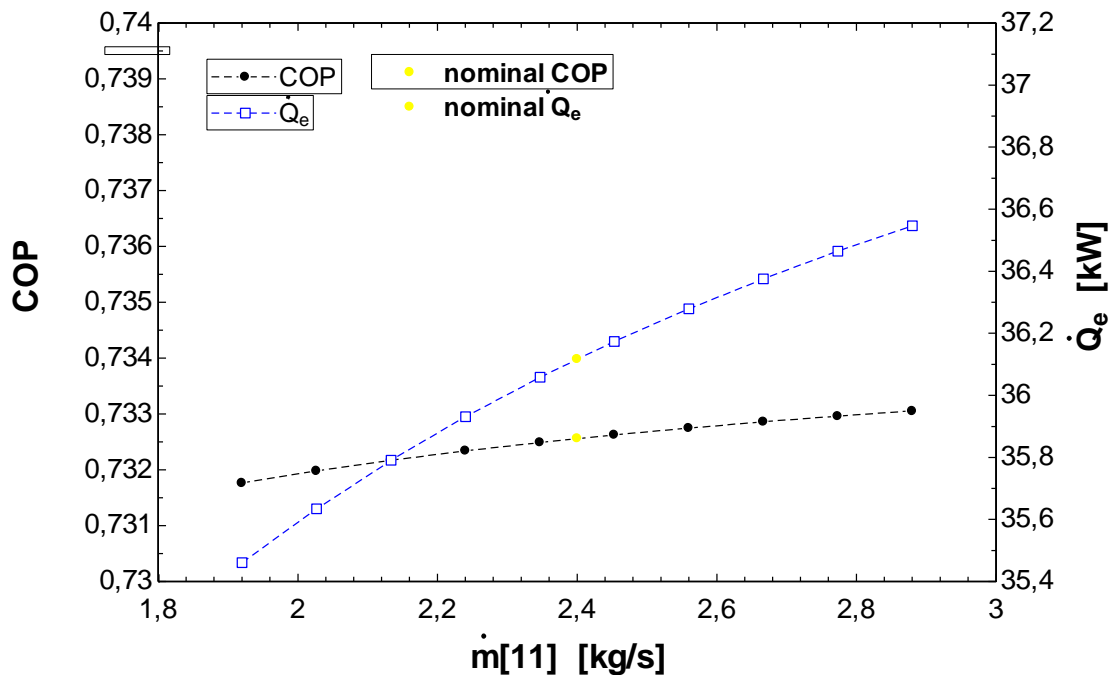


Figure 2: COP; \dot{Q}_E versus \dot{m}_{11}

In the graph of Fig. 2, the hot water flow rate varied from 80% until 120% of nominal flow rate, as the manufacturer datasheet recommends. It can be seen that the coefficient of performance (COP) and the heat removed (\dot{Q}_E) increases as the hot water flow

rate increases. Thus, the highest COP and heat removed (\dot{Q}_E) is achieved for the hot water flow rate value of 2,88 kg/s (120% of nominal flow rate). In the Fig. 3 is plotted the graph COP versus cooling water flow rate (\dot{m}_{13}).

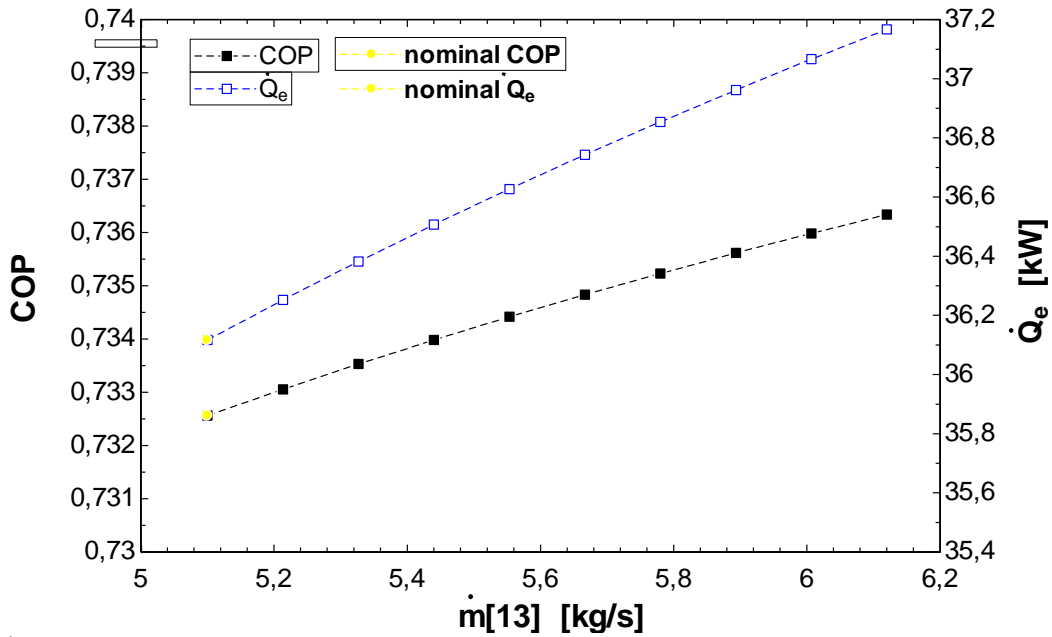


Figure 3: COP; \dot{Q}_E versus \dot{m}_{13}

In the graph of Fig. 3, the cooling water flow rate varied from 100% until 120% of nominal flow rate, as the manufacturer datasheet suggests. It can be observed that the coefficient of performance (COP) and the heat removed (\dot{Q}_E) increase as the cooling water flow rate increases. Thus, the highest COP and heat removed is achieved for the cooling water flow rate value of 6,12 kg/s (120% of nominal flow rate). In this graph the COP and the heat removed (\dot{Q}_E) achieve higher values than the graph in Fig. 2. Therefore, the increase of the cooling water flow rate provides higher COP and heat removed than the increase of hot water flow rate. In the Fig. 4 is plotted the graph COP versus cooling water flow rate (\dot{m}_{17}).

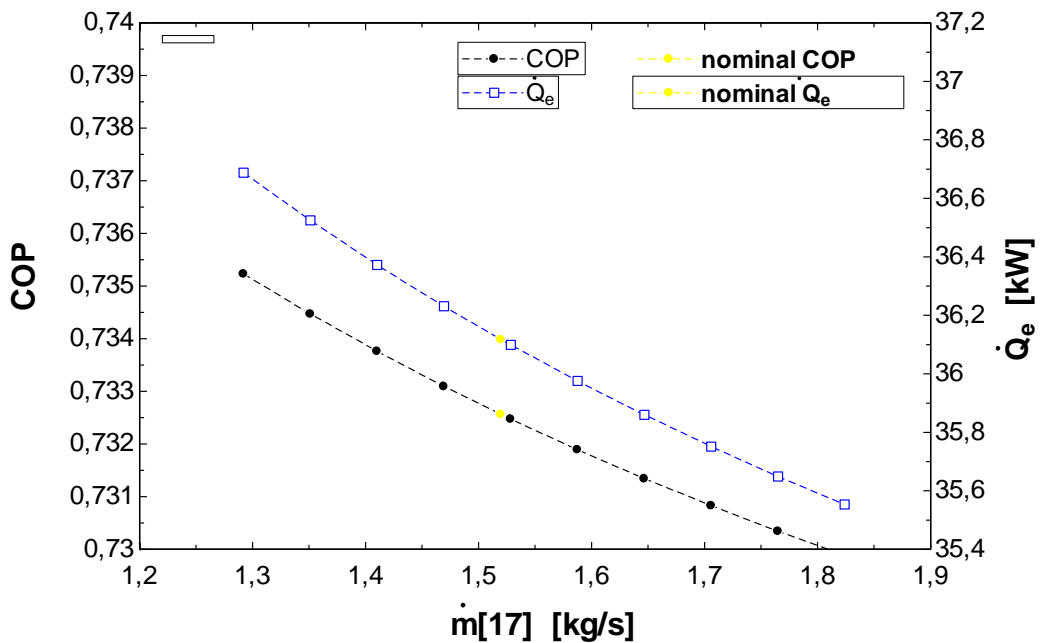


Figure 4: COP; \dot{Q}_E versus \dot{m}_{17} .

In the graph of Fig. 4, the chilled water flow rate varied from 80% until 120% of nominal flow rate, as the manufacturer datasheet recommends. It can be seen that the coefficient of performance (COP) and the heat removed (\dot{Q}_E) decrease as the chilled water flow rate increases. Thus the highest COP and heat removed is achieved for the chilled flow rate value of 1,22 kg/s

(80% of nominal flow rate). In this graph the COP and the heat removed (\dot{Q}_E) achieve higher values than the graph in Fig. 2 however these values are lower than the obtained in the graph of Fig. 3. Therefore, the decrease of the chilled water flow rate provides higher COP and heat removed than the increase of hot water flow rate and lower than the increase of cooling flow rate.

The graph of COP versus T₁₁ (chiller hot water inlet temperature) shows the behavior of the coefficient of performance when the chiller hot water inlet temperature varies as can be seen in the Fig. 5.

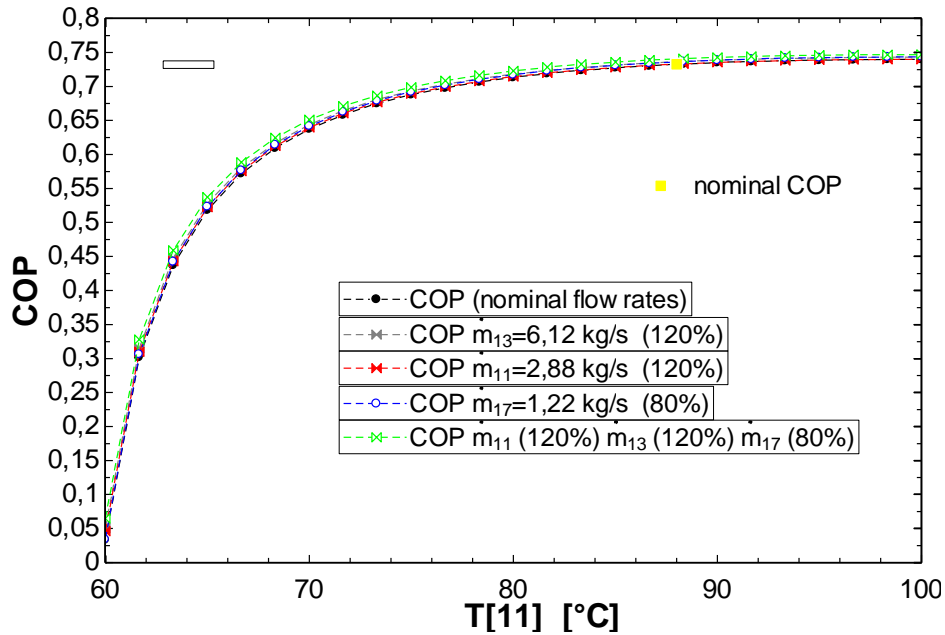


Figure 5: COP x T₁₁.

The curves of Fig. 5 shows that the increase of the hot water inlet temperature (T₁₁) provides higher values of coefficient of performance (COP). The COP increasing rate is higher for lower values of T₁₁ and when the hot water inlet temperature is higher than 80°C, the coefficient of performance almost don't increases. For the different flow rate conditions, the graph presents that the COP varies few when the external flow rates vary. In this graph, the highest value of COP for each hot water inlet temperature (T₁₁) is obtained for the all external flow rates configurations that achieves the best performance of the chiller (120% of nominal flow rate for \dot{m}_{11} and \dot{m}_{13} , and 80% of nominal flow rate for \dot{m}_{17}). Fig. 6 presents the graph of heat removed (\dot{Q}_E) versus T₁₁.

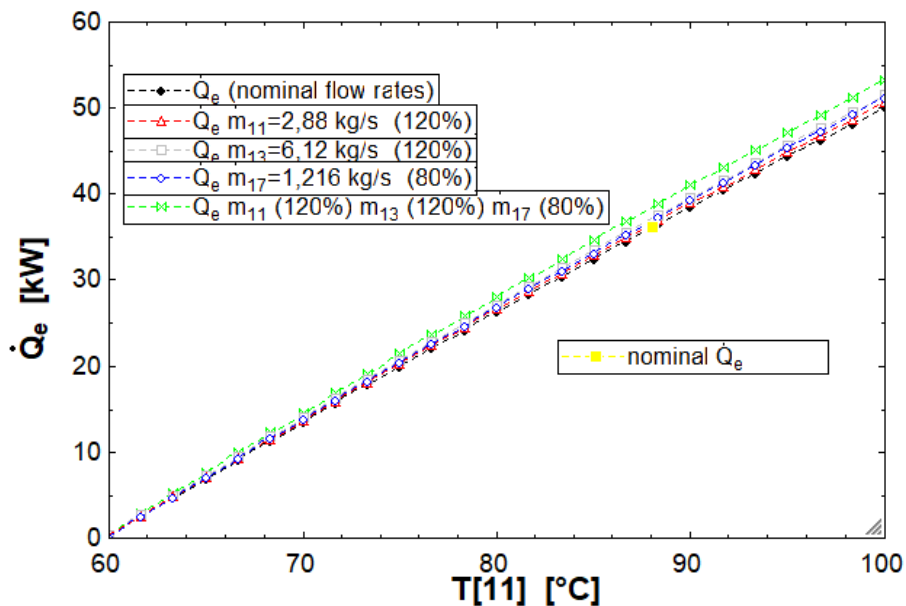


Figure 6: \dot{Q}_E x T₁₁.

The graph of Fig. 6 shows that the increase of the hot water inlet temperature (T₁₁) provides higher values of heat removed (\dot{Q}_E). The heat removed increases as the hot water inlet temperature increases and the maximum value of T₁₁ achieves the highest

value of \dot{Q}_E in this graph. Higher values of T_{11} provides higher differences between the heat removed values of the different external flow rates configurations. In this figure, the highest value of \dot{Q}_E for each hot water inlet temperature (T_{11}) is obtained for the all external flow rates configurations that achieves the best performance of the chiller (120% of nominal flow rate for \dot{m}_{11} and \dot{m}_{13} , and 80% of nominal flow rate for \dot{m}_{17}).

The behavior of the COP and heat removed varying the cooling water inlet temperature (T_{13}) can be also observed by graphs. Fig. 7 present the curves of COP versus T_{13} .

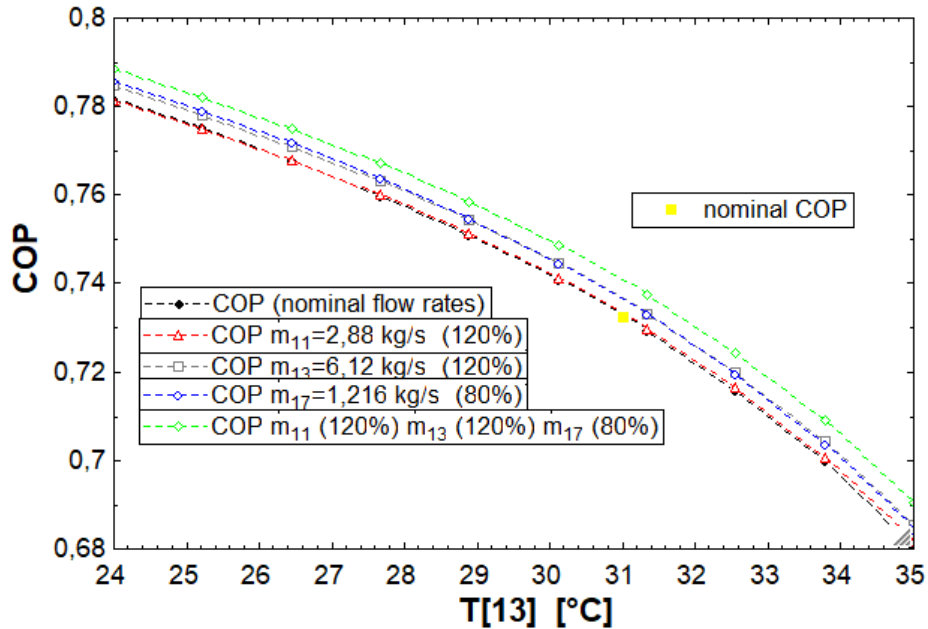


Figure 7: COP x T_{13} .

In fig. 7 can be seen that the more cold the inlet cooling water is, the higher is the coefficient of performance (COP). It is observed in this figure that when only the hot water flow rate varies, the COP improvement from the nominal flow rates is very small. When the absorption system is with 120% of nominal cooling water flow rate or 80% of nominal chilled water flow rate, these resulting COP values are close. The highest COP in this graph is obtained for the all external flow rates analyzed configurations that achieves the best performance of the chiller (120% of nominal flow rate for \dot{m}_{11} and \dot{m}_{13} , and 80% of nominal flow rate for \dot{m}_{17}). This graph shows that for T_{13} below than 29°C it can be achieved higher COP than is observed in fig. 6, which presents T_{11} variation until 100 °C. Fig. 8 presents the curves of heat removed (\dot{Q}_E) versus cooling water inlet temperature (T_{13}).

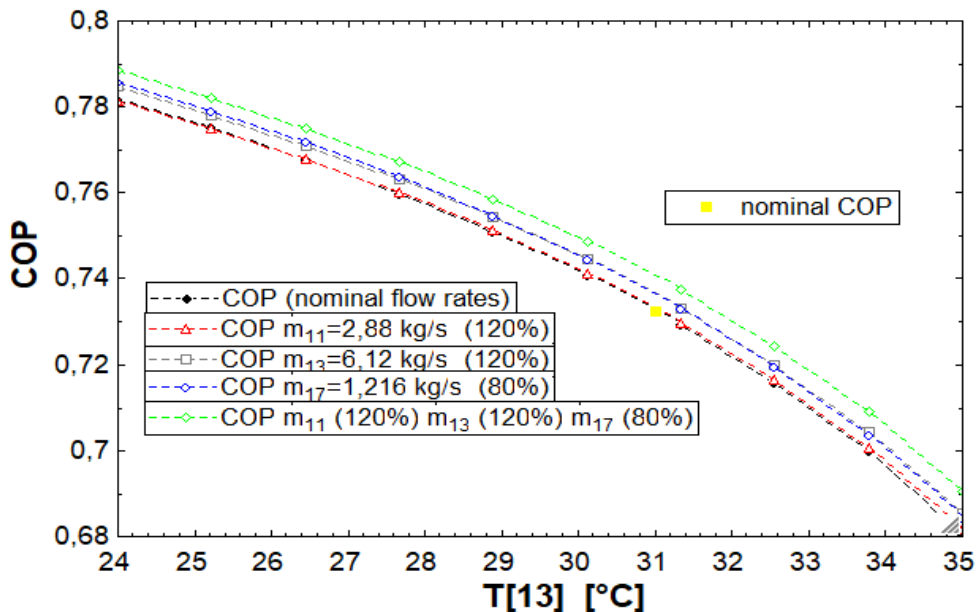


Figure 8: \dot{Q}_E x T_{13} .

In figure 8 is observed that the colder is the inlet cooling water temperature (T_{13}), the higher is the heat removed (\dot{Q}_E). The difference between the values of heat removed in this figure is small except in the best flow rates configuration (120% of nominal flow rate for \dot{m}_{11} and \dot{m}_{13} , and 80% of nominal flow rate for \dot{m}_{17}) which reaches the highest value of \dot{Q}_E . If the inlet cooling water temperature (T_{13}) is 24°C, the heat removed is higher than the highest heat removed found in fig. 7 varying the hot water inlet temperature.

CONCLUSION

A thermodynamic modelling of a 10 TR single-effect absorption chiller was done using the equations of mass, energy and species balance and different graphs were plotted to analyze the behavior of the absorption chiller in different flow rates and inlet water temperatures conditions.

In the flow rate range allowed by the chiller manufacturer datasheet, it was seen that the best configuration is with 120% of nominal flow rate for \dot{m}_{11} (hot water) and \dot{m}_{13} (cooling water), and 80% of nominal flow rate for \dot{m}_{17} (chilled water). The chiller performance enhances when \dot{m}_{11} or \dot{m}_{13} increases, or \dot{m}_{17} decreases, achieving higher heat removed (\dot{Q}_E) and coefficient of performance (COP).

Higher inlet hot water temperature (T_{11}) or lower inlet cooling water temperature (T_{13}) provides the best performance of the chiller, reaching also higher COP and heat removed values. It was observed that if the inlet cooling water temperature is 24 °C, the chiller performance is even better than with an inlet hot water temperature of 100 °C.

All the graphs plotted from the modelling developed present the behavior of the chiller in different flow rates configurations in different inlet hot and cooling water temperatures. Therefore, the modelling allows to analyze the chiller performance providing a better understanding of the external flow rates impacts in an absorption refrigeration system.

ACKNOWLEDGEMENTS

The first author would like to thank CAPES for the Master's scholarship. The second author would like to thank FACEPE for the scientific research scholarship.

REFERENCES

- Chahartaghi, M., Golmohammadi, H., Shojaei, A. (2019). Performance analysis and optimization of new double effect lithium bromide-water absorption chiller with series and parallel flows. *International Journal of refrigeration*, Vol. 97, pp. 73-87.
- Engineering Equation Solver (EES). F-Chart Software, LLC.
- Lee, S., Lee, J., Lee, H., Chung, J., Kang, Y. (2019). Optimal design of generators for H₂O/LiBr absorption chiller with multi-heat sources. *Energy*, Vol. 167, pp. 47-59.
- Meyer, T., Ziegler, F. (2019). A characteristic mass fraction difference in absorption chillers. *International Journal of Refrigeration*, Vol. 97, pp. 67-72.
- Srikhirin, P., Aphornratana, S., Chungpaibulpatana, S. (2001). A review of absorption refrigeration technologies. *Renewable and Sustainable Energy Reviews*, Vol. 5, pp. 343-372.